Food Hydrocolloids 155 (2024) 110174

Contents lists available at ScienceDirect

Food Hydrocolloids

journal homepage: www.elsevier.com/locate/foodhyd

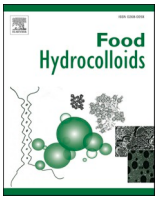

Mung bean protein colloid mixtures and their fractions - A novel and excellent foam stabiliser

Qiuhuizi Yang [a,1], Jack Yang [a,1], Babet Waterink [a], Paul Venema [a], Renko de Vries [b], Leonard M.C. Sagis [a,*]

[a] Laboratory of Physics and Physical Chemistry of Foods, Wageningen University, Bornse Weilanden 9, 6708WG, Wageningen, the Netherlands
[b] Laboratory of Physical Chemistry and Soft Matter, Wageningen University, Stippeneng 4, 6708, WE, Wageningen, the Netherlands

ARTICLE INFO

Keywords:
Mung bean protein
Dry fractionation
Protein coacervates
Interfacial rheology
Foam stability
Plant protein microgels

ABSTRACT

Protein aggregates are known to enhance foam stability by either increasing the thin film viscosity or by blocking the lamellae of a foam. In this study, we produced a mung bean protein colloids mixture (MPCM) by heating protein coacervates that were formed by liquid-liquid phase separation. The functionality of MPCM was compared to a mildly purified mung bean protein extract (MIL). The MPCM showed extraordinary foaming properties, much better than MIL, with foamability of 324 % and a half-life time of 400 min. This work focused on elucidating the exact interface and foam stabilising mechanism of the MPCM by separating the colloids (COL) from the supernatant/continuous phase of the MPCM (SUP). Their interfacial properties were studied by performing surface dilatational rheology and microstructure analysis. Finally, foaming properties, such as foamability, foam stability, and air bubble size, were studied.

It was found that the highest foam capacity was observed for the SUP fraction by generating stiffer interfaces. This fraction also contributed to the high foam stability of the MPCM. The COL fraction was found to form a viscoelastic thin film between air bubbles, thereby decreasing the drainage rate of the foam. In brief, SUP and COL fractions co-operate in the formation of highly stable MPCM foam, leading to a promising plant-derived candidate for producing stable foams in food products.

1. Introduction

As an alternative to animal-based proteins, plant-based proteins have received considerable attention in terms of their techno-functionalities. Besides the currently prevalent topic of meat analogues, plant-based proteins are also considered as foaming agents or emulsifiers, as a replacement for dairy or egg proteins. Among these alternatives, mung bean is an upcoming and promising plant-based protein source (Wang et al., 2022; M. Yang, Faber, et al., 2021). The main reasons for this rising interest are sustainability aspects and the well-balanced amino acid composition (Hou et al., 2019) of mung bean proteins. In terms of sustainability, mung bean can be cultivated with low water usage and without nitrogen fertilizers (Iriti & Varoni, 2017). In addition, it is widely cultured not only in traditional mung bean-consuming countries (Asia), but also in Southern Europe and Northern America.

For replacing animal proteins in foaming applications, the main focus is currently still on soybean and pea proteins. Unfortunately, both of these sources have an interfacial behaviour that is inferior compared to animal-derived proteins. The foaming capacity of these plant-based proteins was observed to be lower (Brishti, Zarei, Muhammad, & Saari, 2017; Kornet et al., 2022; Ma et al., 2011; Xia et al., 2022) than whey protein isolates, in many cases (Nicorescu et al., 2009; J. Yang, R. Kornet et al., 2022). For mung bean proteins, few investigations have been conducted on their interfacial stabilising properties. They were found to have better foam capacity but lower stability than soybean protein (Brishti, 2017; Liu et al., 2022).

It has been shown that mild processes can produce plant-based protein ingredients with better functionalities compared to classical extraction methods, such as acid precipitation (Assatory et al., 2019; Kornet et al., 2022; Pelgrom et al., 2015; J. Yang, I. Faber et al., 2021; Q. Yang, Berton-Carabin, et al., 2022). Nevertheless, extensive processing has not always led to worse functional behaviour. Heating-induced colloids and aggregates were found to increase the stability of protein-stabilised foams. So far, the majority of these studies focus on

* Corresponding author.
E-mail address: leonard.sagis@wur.nl (L.M.C. Sagis).
[1] co-first author.

https://doi.org/10.1016/j.foodhyd.2024.110174
Received 16 February 2024; Received in revised form 30 April 2024; Accepted 8 May 2024
Available online 9 May 2024

the thermal aggregation of animal-based globular proteins due to their high solubility (Nicolai, 2016). Aggregates of whey protein isolates (Nicorescu et al., 2009, 2010; Schmitt et al., 2007), whey protein microgels (Nicolai, 2016), casein micelles (Chen et al., 2018), and β-lactoglobulins (Rullier et al., 2008, 2009, 2010) were extensively studied at both acidic and neutral pH. In these studies, the supramolecular structures could only form foams with high stability in the presence of a sufficient amount of non-aggregated proteins. Based on these studies, aggregates have been revealed to enhance foam stability in two ways: either by increasing the viscosity of the thin films between air bubbles, or by blocking the lamellae or plateau borders, resulting in slowing down the drainage rate and leading to more stable foam (Chen et al., 2018; Rullier et al., 2008, 2009). Aggregation does not always lead to improved foaming properties: when aggregates become too large (>1 μm), they often appear to be detrimental for the foaming properties, and can act as anti-foamers. While aggregated proteins are widely studied for their foaming properties, the exact role of each of the individual fractions of these mixtures of plant-based aggregates and non-aggregated material in the stabilisation of foams has not received as much attention, especially for mung bean protein-stabilised foams.

Soybean protein is a typical plant-derived protein which has been extensively studied in terms of its functionalities. By heating soybean protein isolates at various temperatures from 80 °C to 100 °C, Guo et al. (2015) produced soluble aggregates of medium-size (670–1000 kDa) and large-size (>1000 kDa). Medium-size aggregates appeared essential to enhance foaming capacity due to a supportive effect provided by their loose structure, while a large proportion (>50%) of large-size aggregates presented would form films with increased thickness, leading to increased foam stability. This improvement in foam stability could result from the thin film stabilisation mechanism mentioned before.

Except for aggregate size, the impact of protein composition and processing on foam stabilising properties of aggregates has also been investigated. The effect of heating and drying on foam properties of heat-induced pea protein aggregates was evaluated at both acidic and neutral pH (J. Yang, H. C. M. Mocking-Bode et al., 2022). It was shown that independent of drying methods, the pea protein aggregates formed stiffer layers than the native proteins.

Previously, mung bean protein colloids were produced by adjusting the pH of mung bean protein solutions to induce liquid-liquid separation, followed by heating (Yang et al., 2023; Yang et al., 2022). These colloids are suitable for producing high-protein beverages, due to their high internal protein content, low intrinsic viscosity and weak heat-induced gelation behaviour (Q. Yang, Yang, et al., 2023). An extraordinary interfacial behaviour was observed in our previous study as well. The colloidal mung bean protein dispersions formed exceptionally stable foams (half-life time around 400 min) with high foam capacity (overrun around 325%), and this is dramatically higher than foam stabilised by pea protein aggregates, which showed a half-life time of approximately 4 min. Mung bean protein colloids can generate foams with even higher stability than whey protein isolates, which presented a half-life time around 260 min (J. Yang, S. P. Lamochi Roozalipour et al., 2021). However, the reasons for such an excellent foaming behaviour of mung bean protein colloids are still unknown. Since functionality of plant-based proteins can differ significantly from source to source, the role of the different fractions present in dispersions of thermally-induced plant protein aggregates in foam stabilisation still needs to be validated for legumes other than yellow pea and soybean. The mung bean protein colloids prepared by simple coacervation can be considered microgels or nanogels and could be used as fat replacers or for encapsulation and targeted delivery in the food systems (Inthavong et al., 2019; Sandoval-Castilla et al., 2004; Sağlam et al., 2013; Shewan & Stokes, 2013). Exploring the foam stabilisation mechanism of mung bean protein colloids could potentially expand their application range.

Hence, in the present study, we determined the stabilising mechanism of mung bean protein colloids mixtures (MPCM) and the role of the aggregated and non-aggregated fractions in these mixtures in foam stabilisation. The interfacial behaviour, including adsorption rate, surface oscillatory dilatational rheology and surface microstructure of the mixture and fractions were investigated. Also, the foaming properties, including foam capacity, foam stability and air bubble size, were also measured. Our results show the potential of MPCM to be developed into a sustainable and highly functional plant-protein foaming agent in food systems.

2. Experimental section

2.1. Materials

Dry mung bean seeds (Golden Chief, Thailand) were purchased from the online Asian store MyEUShop (Nieuw-Vennep, The Netherlands). All chemicals (Sigma-Aldrich, USA) were used as received. The solutions were prepared in ultrapure water (MilliQ Purelab Ultra, Darmstadt, Germany).

2.2. Sample preparation

2.2.1. Preparation of mung bean protein colloids

A mung bean protein fine fraction (FF) was obtained by dry fractionation, as described earlier (Yang, Berton-Carabin, et al., 2022). A 20% wt. suspension was produced by dispersing the FF fraction in 15 mM sodium metabisulfite solution, where the pH of the suspension was adjusted to 8.5 using 1M NaOH. After 1h stirring at room temperature, the suspension was centrifuged at 10,000g for 30 min to remove starch granules and insoluble fragments, and the supernatant was collected. Afterwards, the pH of the supernatant was adjusted to 6.75 to induce the formation of liquid (nearly) spherical protein coacervates. The proteins in the coacervates were cross-linked by a heating step at 80 °C for 20 min, while stirring to obtain the so-called mung bean protein colloids mixture (MPCM). Subsequently, the MPCM were freeze-dried to be used for further investigations.

2.2.2. Preparation of a mild mung bean protein extract

Additionally, FF was dispersed in water in a 1:10 (w/w) FF/water ratio and stirred for 2 h, followed by adjusting pH to 8.5 using 1 M NaOH solution and a centrifugation step at 10000g for 30 min to remove the starch granules and cellular debris. The supernatant was collected and freeze-dried, which resulted in a mildly purified protein mixture (MIL).

2.2.3. Fractionation of mung bean proteins and colloids

All samples were prepared based on weight-based protein content (% w/w) in a 20 mM PO_4-buffer, pH 7.0, while stirring for at least 4 h at room temperature. Samples were prepared in a protein concentration range from 0.1 to 1.0% (w/w). In order to obtain different fractions, a 1% MPCM suspension was prepared and centrifuged at 20000g for 30 min. The supernatant from the first centrifugation step was obtained as a sample and referred to as supernatant (SUP). The weight of this SUP solution was recorded. A buffer was added to resuspend the pellet, and the centrifugation and washing steps were repeated three times to obtain the purified pellet (COL) finally. In the final washing step, we added the same amount of buffer as the weight of the SUP solution. More details are presented in Fig. 1.

2.3. Size exclusion chromatography

Size exclusion chromatography (SEC) was carried out by an ÄKTA pure 25 system (Cytiva, Marlborough, MA, USA) equipped with Superdex® 200 10/300 GL column. Protein solutions with protein concentrations of 0.1% (w/w) were centrifuged at 15000 g for 10 min. Subsequently, 50 μL supernatant was injected into the system with sodium phosphate buffer (20 mM, pH 7.0) containing 50 mM NaCl as the eluent. The flow rate was set at 0.5 mL/min and the elution was recorded with UV absorbance at 280 nm.

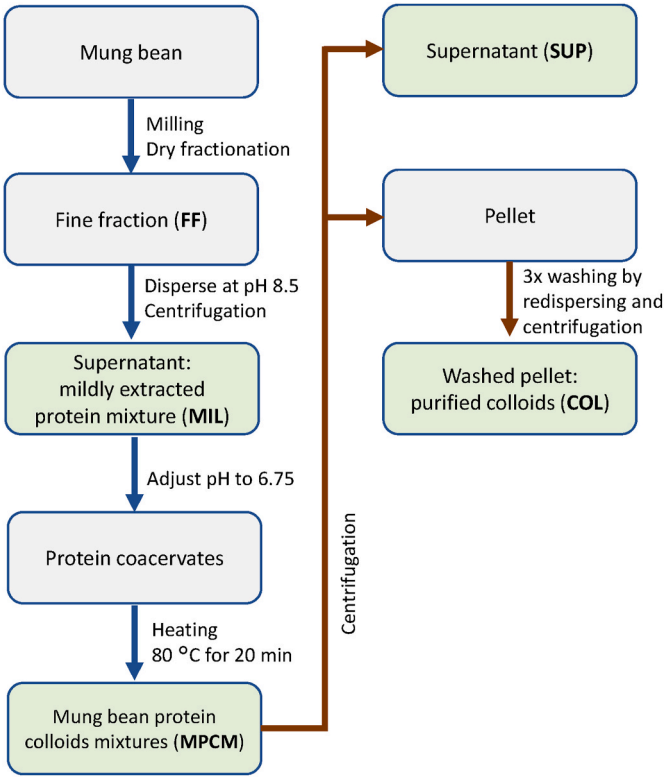

Fig. 1. Schematic overview of the sample fractionation.

2.4. Determination of particle size

The particle size distribution was analysed using dynamic light scattering (Zetasizer Nano ZS, Malvern Instruments Ltd., UK). Dispersions with 0.1 % (w/w) protein were injected in a DTS1070 Zetasizer cell. Prior to analysis, the sample cell was equilibrated for 2 min at 20 °C, followed by a size distribution measurement, where 12 scans were performed in automatic mode, of which an average was calculated. All measurements were at least performed in triplicate.

2.5. Determination of protein surface hydrophobicity

The protein surface hydrophobicity was determined using 8-anilino-1-napthalenesulfonic acid ammonium salt (ANSA) as a fluorescence agent (Esmaeili et al., 2015). MPCM fractions were dispersed in a phosphate buffer at protein concentrations varying from 0.005 to 0.04 % (w/w). Protein dispersions were loaded in double-sided transparent plastic cuvettes, and 25 μL of 8 mM ANSA solution was added to each cuvette. Next, the samples were mixed using a vortex mixer and incubated for 1 h in a dark environment to prevent deterioration of the ANSA reagent. After incubation, the fluorescence of samples was determined by an LS 50B luminescence spectrometer (PerkinElmer, USA), the excitation wavelength was 390 nm, and the emission wavelength was set at 470 nm. The buffer solution was used as a blank. The initial slope of the fluorescence intensity versus protein concentration was used to measure surface hydrophobicity (H_0). The relative surface hydrophobicity was calculated to compare hydrophobicity among the samples. All samples were studied in triplicate.

2.6. Determination of surface tension and surface dilatational properties

The mechanical properties of the air-water interface were studied by performing surface dilatational rheology in a drop tensiometer PAT-1M (Sinterface Technologies, Germany). A 0.1 % (w/w) protein solution was used to form a hanging droplet with a surface area of 20 mm^2 at the tip of a hollow needle. The surface tension was calculated by fitting the Young-Laplace equation to the shape of the droplet. Two types of oscillatory deformation measurements were performed, and prior to the start of each of these analyses, the droplets were equilibrated for 10800 s, to allow for adsorption of the protein and obtain an (almost) constant surface tension, thus giving us a stable baseline for the oscillatory deformations. Frequency sweeps were performed at a constant amplitude of 3%, in a frequency series, which increased from 0.002 to 0.1 Hz. Amplitude sweeps were performed at a constant frequency of 0.02 Hz, in an amplitude series, which increased from 3 to 30% deformation amplitude. In these oscillatory deformations, five cycles were performed for each frequency or amplitude step. All measurements were performed at least in triplicate at 20 °C.

2.7. Rheology data analysis

The raw data of the amplitude sweeps were transformed into Lissajous plots by plotting the surface stress (γ-γ_0) against the deformation ($(A\text{-}A_0)/A_0$). Here, γ and A are the surface tension and area of the deformed interface, and γ_0 and A_0 are the surface tension and area of the non-deformed interface. The plots were generated using the middle three of five oscillations.

2.8. Preparation of Langmuir-Blodgett films

Langmuir-Blodgett films of the interfacial films were created using a Langmuir trough (243 mm^2 Langmuir-Blodgett Trough KN 2002; KSV NIMA/Biolin Scientific Oy, Finland). First, the trough was filled with the subphase, a 20 mM PO_4 buffer at pH 7.0. The surface was carefully cleaned using a vacuum pump. Afterwards, 200 μL of 0.1 % protein (w/w) solution of MIL and MPCM was injected at the bottom of the trough using a gas-tight syringe. The proteins were allowed to adsorb at the interface for 10800 s, while the surface pressure was monitored using a Wilhelmy plate (platinum, perimeter 20 mm, height 10 mm). After the waiting period, the interface was compressed by Teflon barriers at a moving speed of 5 mm/min. The interfacial films were compressed to a target surface pressure of 15 or 25 mN/m, and the protein film was deposited on a freshly cleaved mica substrate (Highest Grade V1 Mica, Ted Pella, USA) using Langmuir-Blodgett deposition at a withdrawal speed of 1 mm/min. The Langmuir-Blodgett films were dried for two days and were further analysed using atomic force microscopy. All films were produced in duplicate at 20 °C.

2.9. Determination of the interfacial structure by AFM

Atomic force microscopy (AFM) was applied to study the topography of the interfacial microstructure of Langmuir-Blodgett films. The AFM (Multimode 8-HR, Bruker, USA) was equipped with a Scanasyst-air model non-conductive pyramidal silicon nitride probe (Bruker, USA) with a normal spring constant of 0.40 mN/m. The films were recorded in tapping mode at a lateral frequency of 0.977 Hz, and an area of 2 × 2 μm^2 was analysed with a lateral resolution of 512x512 $pixels^2$. All films were recorded at least two locations to ensure good representativeness, and the images were analysed using Nanoscope Analysis software v1.5 (Bruker, USA).

2.10. Determination of foam properties

2.10.1. Ability and stability of foams created by whipping

Foams were created by whipping 15 mL of 0.1–1.0 % protein (w/w) solutions with an overhead stirrer equipped with an aerolatte foam head at 2000 rpm for 2 min in a plastic container (34 mm diameter). The foamability was determined by marking the bottom and upper level of the foam, of which the height was measured and recalculated into the maximum foam volume using the radius of the container. From this, the overrun was calculated using equation 1.

$$Foam\ overrun\ (\%) = \frac{Maximum\ foam\ volume\ (mL)}{Initial\ solution\ volume\ (15\ mL)}\ x\ 100\ \%$$

After determining the maximum foam volume, the foam sample was transferred into a 50 mL volumetric glass cylinder. The liquid and foam height of the sample was determined from 1 min after foam formation, until the foam volume decayed by half. All measurements were performed in triplicate at 20 °C.

2.10.2. Stability of foams created by sparging

Sparged foams were created in a Foam scan foaming device (Tecles IT-concept, France). A glass cylinder (60 mm diameter) was filled with 40 mL of sample, and gas was sparged through a metal frit (27 μm pore size, 100 μm distance between centres of pores, square lattice) at a 400 mL/min flow rate. The generated foam in the tube was studied by image analysis to obtain a foam volume, and the foams were sparged to a volume of 400 mL. Afterwards, the foam volume was monitored until a 50 % decay of volume, which is known as the foam volume half-life time. A second camera recorded a detailed image of the air bubbles, which was analysed using a custom Matlab script with a DIPlip and DIPimage analysis software package (TU Delft, NL) to determine an average bubble size. All experiments were at least performed in duplicate at 20 °C.

3. Results and discussion

3.1. Characterization of the different protein fractions

Our previous study showed a superior foam capacity and stability for mung bean protein colloid mixtures (MPCM) (J. Yang, Yang, et al., 2023). In order to reveal the mechanism behind this observation, MPCM were fractionated into a supernatant (SUP) and colloid (COL) fraction by centrifugation, several washing steps and redispersing. The protein content and dry matter content of these fractions were determined. As shown in Table 1, the majority of proteins in MPCM ended up in SUP, and consequently led to a higher dry matter content for SUP.

SEC (size exclusion chromatography) was performed to investigate the protein composition of the MIL and SUP fractions. As shown in Fig. 2, in MIL a small peak for legumin was observed at an elution volume of 11 mL, representing proteins with a molecular weight of 660 kDa. A major peak for vicilin (around 12 mL, 261 kDa) and albumin (around 14.5 and 16 mL, 113 and 35 kDa, respectively) were observed in MIL, while a very small peak for vicilin was observed in SUP. The absence of legumin and extremely low amount of vicilin in SUP suggested that most of these proteins ended up in COL. A similar observation was reported by Kornet, Roozalipour, et al. (2022), where most of the vicilin remained in the continuous phase, while most of the legumin (approx. 70 %) was found in the coacervates of pea and soy proteins. The SEC results imply that the protein composition in coacervates of legume proteins are dominated by the legumin protein fraction.

The particle size distribution of MPCM fractions and mildly purified MB protein mixtures (MIL) were obtained from dynamic light scattering and presented in Fig. 3. The MIL sample showed the smallest average diameter around 10 nm, attributed to the mild purification method, which avoided extensive aggregation. SUP was found to have a peak at 30 nm and a shoulder between 50 and 700 nm. COL showed the largest average diameter around 1000 nm, while MPCM showed a particle size distribution between SUP and COL, as expected. The average size of MPCM is around 150 nm, and a second peak around 10^5 nm was also observed. This peak represents a small number of aggregates and can be neglected based on the volume distribution.

The protein foam-stabilising properties may be largely impacted by protein surface properties such as hydrophobicity. As an index of the number of hydrophobic groups on the surface of proteins, the relative protein surface hydrophobicity (H_0) was determined using ANSA. As shown in Table 2, COL seems to dominate the H_0 of MPCM since they show comparable hydrophobicity with values of 0.96 and 1.0, respectively. COL showed a relative hydrophobicity higher than SUP, indicating more surface-exposed hydrophobic groups for COL. These MPCM fractions showed significantly higher hydrophobicity values than mildly processed MIL samples. This could be attributed to heat-induced structure alteration during the protein coacervate cross-linking step. These heat-induced increases in surface hydrophobicity have been reported widely by previous researchers for soybean proteins (Shen & Tang, 2012; Wang et al., 2014).

Table 1
Protein content and dry matter of supernatant and pellets fractionated from mung bean protein colloids solutions. The amount of protein and dry matter is expressed as a percentage over the total amount of protein or dry matter in the MPCM.

	Amount of protein(%)	Amount of dry matter(%)
SUP	67.2 ± 2.3	72.1 ± 0.3
COL	32.8 ± 2.3	27.7 ± 0.5

3.2. Interfacial properties of MB fractions

3.2.1. Adsorption behaviour

Since foams normally form on a short time scale (a couple of seconds), the adsorption behaviour of proteins to the interface is an imperative factor to be determined. The highest adsorption rate was presented by MIL, and this may be attributed to its smallest particle size, as shown in Fig. 2. The particle size of MPCM is much larger than MIL, yet MPCM showed comparable adsorption behaviour to MIL during the whole process. Egg proteins measured at same conditions in our previous work showed a slower adsorption behaviour with a lag time of 2 s, followed by a surface pressure increase to 17 mN/m after 10,800 s (J. Yang, R. Kornet et al., 2022). In previous results, the presence of smaller non-cross-linked proteins in whey protein colloids dispersion dominated the interfacial properties in that system (Yang et al., 2020). The adsorption behavior of MPCM was therefore compared to that of COL and SUP. The smaller particle size of SUP resulted in a rapid increase in surface pressure in the initial phase (first 30 s) compared to COL, as the proteins in SUP diffused much faster toward the interface. The COL fraction showed a significant lag time, before the surface pressure started to increase. Based on particle size, we would not expect the COL fraction to adsorb spontaneously to the interface. But, the separation between SUP and COL is not perfect, and small amounts of MB proteins will still be present in this sample. Also, the aggregation induced by heating the coacervates does not have a conversion of 100%. So, there are still unbound proteins in the COL particles, and after redispersing them, these may slowly leach out of the particle. It is most likely that these small amounts of unbound proteinaceous material are responsible for the observed adsorption behavior of COL. These unbound proteinaceous material might also result in the higher final surface pressure of MPCM than SUP. Based on this, we can presume that the adsorption behavior of MPCM is dominated by the proteins in SUP. This assumption was further investigated in foam properties tests.

3.2.2. Surface oscillatory dilatational rheology

3.2.2.1. Amplitude sweeps. To gain insight in the stability and strength of the interfacial films upon deformation, amplitude sweeps were performed with a deformation amplitude from 3 % to 30 % at a constant frequency (0.02 Hz). MPCM and SUP showed almost identical behaviours upon increasing amplitudes. The E_d' (dilatational elastic moduli) of both samples decreased from 70 to 37 mN/m approximately, whereas COL had a lower modulus that ranged between 41 and 29 mN/m. This suggests stiffer interfacial films were formed by MPCM and SUP, and weaker layers were obtained from COL. Therefore, SUP is likely to

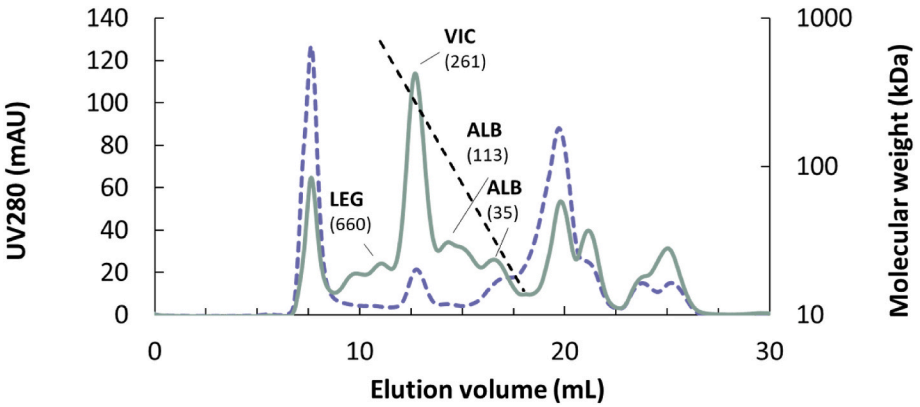

Fig. 2. SEC chromatogram of the 280 nm absorbance as a function of eluted volume of MIL (mildly purified protein mixture, solid green curve) and SUP (supernatant of MPCM, dashed purple curve). The number in rackets represent the molecular weight (kDa) of the corresponding peak. The dashed line represents the calibration curve. The legumin (leg), vicilin (vic) and albumin (alb) peaks are highlighted.

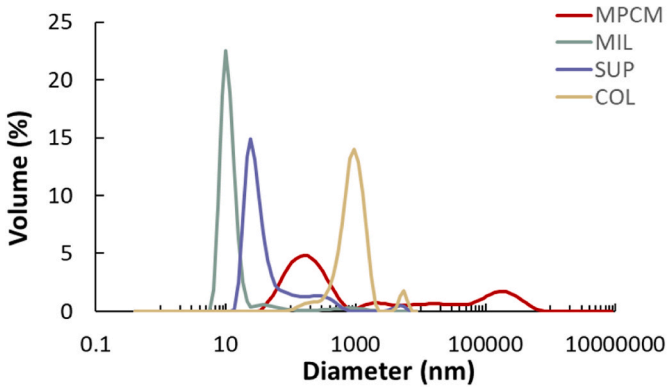

Fig. 3. The size distribution of mung bean protein colloids mixtures (MPCM, red), mildly purified protein mixtures (MIL, green), supernatant of MPCM (SUP, purple) and pellets of MPCM (COL, yellow). All measurements were carried out in triplicate.

Table 2
Relative hydrophobicity of MB protein COL (Pellets) and Sup (Supernatant) fractionated from mung bean protein colloids solutions, and MIL (Mildly purified protein mixtures) obtained from MB fine fraction. The hydrophobicity was calculated based on result of MPCM.

	Hydrophobicity
MPCM	1.00 ± 0.03
COL	0.96 ± 0.03
SUP	0.62 ± 0.02
MIL	0.24 ± 0.01

dominate the dilatational behaviour of MPCM. To investigate the influence of processing on MB protein interfacial behaviour, mildly purified protein mixtures MIL were measured as well. The E_d' of MIL was found to vary between 51 and 29 mN/m, showing a lower dilatational modulus than MPCM. Hence, we conclude that MPCM can form stiffer interfaces than the MIL protein extract.

The moduli obtained for the air-water interface stabilised by MPCM (70–37 mN/m) were approaching the moduli of egg white protein interfacial films, which have Ed' values of 85 to 45 mN/m. In addition, MPCM even had higher moduli than air-water interfacial films stabilised by rapeseed proteins (60–30 mN/m) and globulin-rich fractions of mung bean, yellow pea and Bambara groundnut (51–23 mN/m) (J. Yang, C. C. Berton-Carabin et al., 2022; J. Yang, R. Kornet et al., 2022).

Disruption of the interfacial microstructure caused by deformation could lead to non-linear viscoelastic behaviour. As shown in Fig. 5, all surfaces stabilised by MB fractions are in the NLVE (non-linear regime) as E_d' obviously decreased at higher amplitudes. This implies that higher-order harmonics are present in the Fourier spectrum of the surface stress response. However, the moduli shown in Fig. 5 are obtained based on the first harmonic of the Fourier spectrum, and hence non-linear contributions are neglected. These values are dependable only if deformations are applied in the linear viscoelastic regime. To better analyze the non-linearities, the results of surface stress versus deformation were plotted as Lissajous plots.

3.2.2.2. Lissajous plots. The Lissajous plots of surface stress versus deformation were plotted in Fig. 6. The stress evolution in Lissajous plots is clockwise, where the interfacial area of the MPCM fractions-stabilised interfaces are extended in the upper part of the cycle and are compressed in the lower part of the cycle.

As shown in Fig. 6, all plots are symmetric at 5% deformation, suggesting an almost linear response upon deformation. COL showed a narrower plot, which indicates a more elastic response of the COL-stabilised interface. Other fractions presented wider ellipse shapes, which indicates a relatively higher contribution of the viscous contribution to the response, and a higher energy dissipation upon deformation than COL. The plots of SUP and MPCM were more tilted toward the vertical axis and had higher maximum surface pressure, indicating the formation of stiffer interfacial films than MIL and COL. This is in line with the E_d'-values, as shown in Fig. 5.

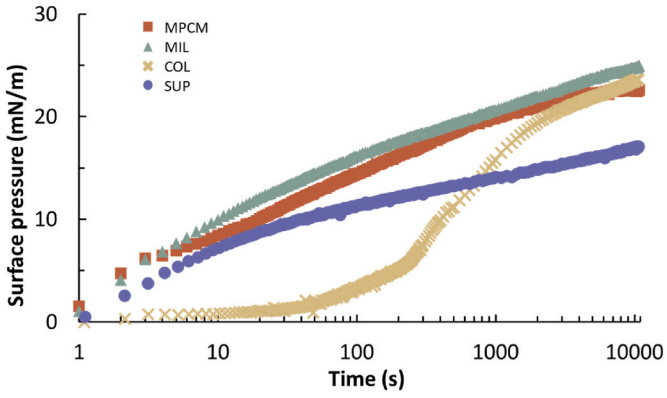

Fig. 4. Surface pressure as a function of time of MPCM (colloids, red squares), MIL (mildly purified protein mixture, green triangles), COL (pellets, yellow crosses) and SUP (supernatant, purple circles). All measurements were conducted at least in triplicate.

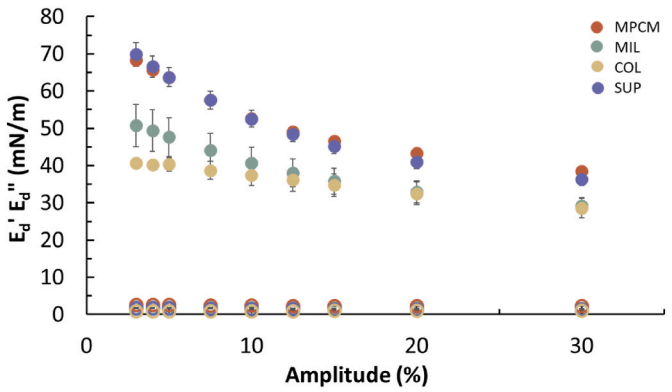

Fig. 5. Surface elastic (E_d', closed symbols) and viscous (E_d'', open symbols) dilatational moduli as a function of deformation amplitude of MPCM (mung bean protein colloids mixture, red), MIL (mildly purified protein mixtures, green), COL (pellets, yellow) and SUP (supernatant, purple). All measurements were conducted in triplicate. Frequency was equal to 0.02 Hz.

When the deformation was increased to 30%, all samples showed significant non-linear behaviour upon deformation, as revealed by their asymmetric plots, except for COL. Relatively steep surface pressure increases were found for MIL, MPCM and SUP at the beginning of the extension phase of the cycle (lower left corner of the plot). Subsequently, the slope of the surface pressure decreased, which indicates intra-cycle strain softening, revealing a gradual disruption of the microstructure. This could be attributed to network disruptions and/or the decrease in the surface density of stabilisers at the interface. The interface is stretched upon extension, and when insufficient additional proteins adsorb to the interface on the time scale of the expansion part of the cycle (~10 s), the surface density decreases, resulting in strain softening. In the compression phase, MIL, MPCM and SUP all presented steep increases in surface pressure upon deformation. The density effect of stabilisers contributes to this phenomenon. It was reported in previous research (Yang et al., 2020) that compression can concentrate stabilisers and generate jammed adsorbed proteins at the interface, leading to intra-cycle hardening in compression.

The presence of softening in extension and hardening in compression can be considered a consequence of in-plane interactions between adsorbed proteins. COL showed obviously different interfacial behaviour from the other samples. The smaller angle with the horizontal axis and the lower degree of asymmetry of the plot suggest that COL formed a weaker and more stretchable film. Moreover, the smaller width of the plots indicates less energy dissipation upon deformation. This observation was supported by an amplitude sweep test, as shown in Fig. 5, where lower moduli were found for COL than MIL, SUP and MPCM. The weak and more stretchable interlayers formed by COL, together with the different adsorption behaviour we saw in Fig. 4, indicate that the colloids themselves are not dominantly present at the interface, and that it is mostly likely that smaller aggregates and other smaller proteinaceous matter have adsorbed at this interface. Comparing SUP and COL, the former appears to dominate in the interfacial behaviour of MPCM.

3.3. *Interfacial microstructure of MB fractions*

To obtain detailed insights into the interfacial microstructure of MPCM and MIL stabilised interfaces, Langmuir-Blodgett films were produced by injecting the protein solutions at the bottom of the trough, followed by compression and deposition. Injection allows the slow diffusion of the surface active components toward the interface, giving a more representative interface compared to the spreading method. Based on surface pressure isotherms, a surface pressure of 15 and 25 mN/m were chosen, which are in the liquid-expanded and liquid-condensed regime, respectively. Finally, the topography of the Langmuir-Blodgett films was analysed using atomic force microscopy (AFM).

The scans of the films are shown in Fig. 7, where higher areas are shown in white, while lower areas are shown in brown. Both MIL and MPCM presented structures with obvious heterogeneity (white dots) at a surface pressure of 15 mN/m, larger and thicker regions were observed in MPCM, indicating more and larger cluster presented in MPCM film. These clusters should be protein clusters, considering the heating process applied during MPCM preparation. This finding is in line with previous report, these clusters were proved to be protein clusters by Sagis et al. (2019). Larger protein clusters presented by MPCM could result from particle size, as larger particles are present in the MPCM than

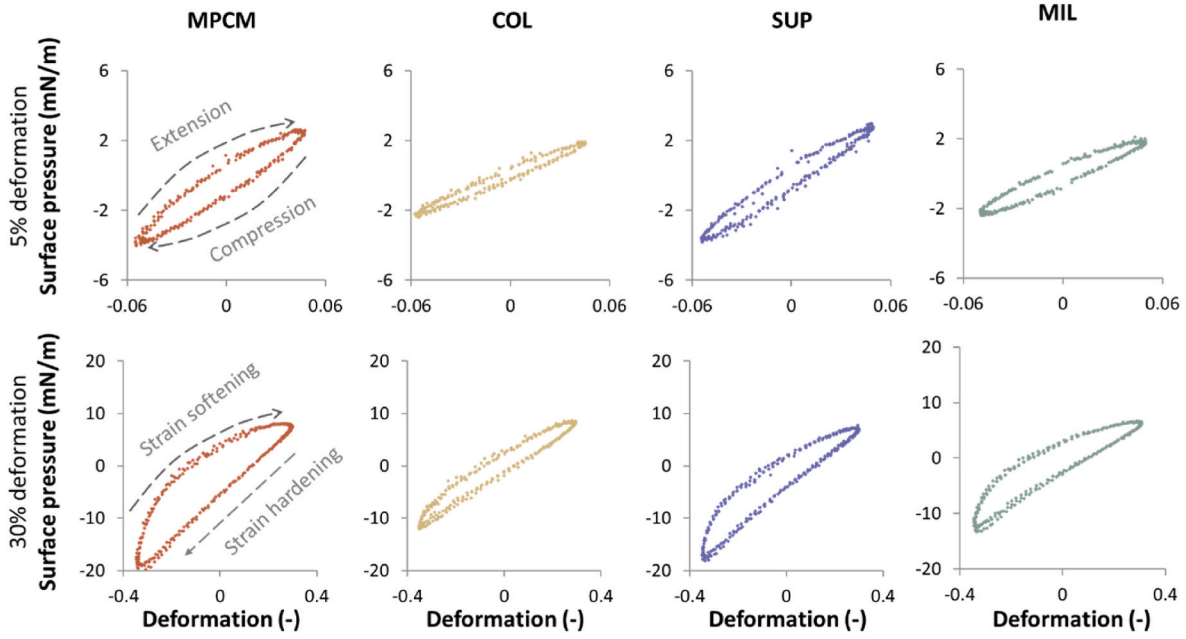

Fig. 6. Lissajous plots of deformation versus surface pressure. The plots are obtained from the amplitude sweeps of the mungbean MIL (mildly purified protein mixture, green), MPCM (mung bean protein colloids mixtures, red), COL (MPCM pellets, yellow) and SUP (MPCM supernatants, purple) stabilised interfacial layers. All measurements were conducted at least in triplicate and one representative plot is presented for each sample. Frequency was equal to 0.02 Hz.

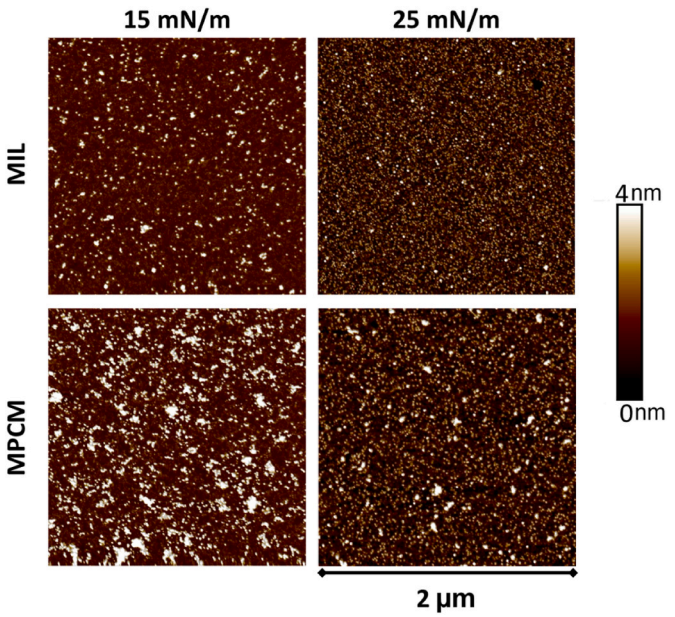

Fig. 7. Atomic Force Microscopy (AFM) images of Langmuir-Blodgett films prepared by MIL (mildly purified mung bean protein mixtures) and MPCM (mung bean protein colloids mixture) stabilised air-water interfaces. The surface pressure designates the conditions applied during the film sampling.

MIL. However, there is no indication that significant numbers of colloids adsorbed at the interface, as these had larger sizes around 1000 nm, according to the DLS results (Fig. 3).

At an increased surface pressure of 25 mN/m, almost similar structures can be observed for both MIL and MPCM. Upon higher compression, fewer large protein clusters were visible whereas more smaller protein dense regions were found, suggesting denser films formed. Similarly dense disordered structures have also been observed for other protein stabilised interfaces, for example, pea proteins (Kornet et al., 2022), rapeseed proteins (J. Yang, I. Faber et al., 2021), and even animal-based proteins such as whey proteins (Rühs et al., 2013) and bovine serum albumin (Sah & Kundu, 2017). MPCM shows a great reduction of large structures upon compression, which may be the result of pushing the material down towards the bulk, making them invisible for a topographical analysis, such as AFM. This observation, together with the results for the adsorption behaviour and dilatational rheology, again shows the dominance of the smaller particles/non-aggregated proteins at the interface, stabilised by MPCM.

3.4. Foam properties

To evaluate the foaming properties of various mung bean protein fractions, the foam overrun, half-life time and air bubble size of the foam were obtained. The foam overrun was determined by whipping the fraction solutions and characterised as the foam volume over the initial solution volume. To evaluate foam stability, foams from different mung bean protein fractions were prepared by sparging, and the 50 % decay time was recorded, and the air bubble size was analysed by a Matlab package. Two different protein concentrations were studied: 0.1 and 1.0% (w/w). These concentrations were chosen, as at 0.1% (w/w) is a concentration in the poor protein regime, where the amount of protein is generally the limiting parameter. At 1.0% (w/w), sufficient proteins are present, and thus the foaming method will be the limiting parameter. Assessing both concentrations could give complementary insights into the foaming properties of the proteins.

3.4.1. Foam capacity

The most considerable increase in overrun was observed for MPCM, which increased vastly from 60 % to 324 % when the protein concentration increased from 0.1 wt% to 1 wt%. The foamability of COL is much lower than that of MPCM, and for the latter, foamability seems to be dominated by SUP. According to Fig. 8, COL can barely make foam itself, as the lowest overrun was observed at both protein concentrations. This could be related to its long lag time in the adsorption process, and as a result, a significantly larger air bubble size was obtained compared to SUP at 1 wt%. At 0.1%, a foam could not be created at all for the COL fraction. At 1%, there was apparently enough smaller material present to create foam, albeit with very large bubble size and very low overrun. The relatively stiffer interfacial layers SUP and MPCM formed can also play a role, as it would slow the coalescence rate of air bubbles, and consequently lead to a higher foam volume. The relatively lower absolute number of oligomers present in MPCM compared to SUP, can explain the higher foam capacity for the latter, although the difference between them at 1% concentration is insignificant. The same finding was previously reported by Kornet et al. (2022) for pea protein fractions. It should be noted that, MIL (mildly purified protein mixture) did not show a better foamability than SUP, although it has a smaller particle size (around 10 nm) than SUP, and a rapid adsorption rate. This behaviour could be attributed to its lower hydrophobicity and lower interfacial layer stiffness.

3.4.2. Foam stability

Foam stability was assessed, in terms of the half-life time for the different mung bean protein fractions. The MPCM showed superior foam stability to others with a foam half-life time of 400 min at 1.0% (w/w). For comparison, such high half-life time could not be reached by whey (300 min) and egg protein (100 min) stabilised foams (J. Yang, R. Kornet et al., 2022). A better foam stability by MPCM can be the result of smaller air bubble size. But no significant difference in bubble size was observed for foams stabilised by the different fractions at 1 % w/w.

As reported previously (Rullier et al., 2008; Saint-Jalmes et al., 2005; Schmitt et al., 2007), two mechanisms can explain the enhanced foam stability in systems containing colloidal particles: either by blocking of the thin films and the Plateau borders by the particles, or by the formation of stiff viscoelastic air-water interfaces. When large particles block the lamellae and Plateau borders, they slow down the drainage and destabilisation of the foam.

COL possessed the largest particle size, but the lowest foam stability of all samples. This system showed very slow adsorption and the resulting interfaces had the lowest stiffness. This indicates the colloids can not stabilize a foam by creating firm viscoelastic interfaces. When comparing the SUP and MPCM foam, both fractions have similar stiffness, and at 1% a similar overrun and bubble size. Yet the half-life time of MPCM is about 3 times longer than that of the foam produced by SUP. And there is less small (non-aggregated) proteinaceous matter in the MPCM sample than in the SUP sample. This indicates that a combined effect of the smaller protein fractions (in SUP) and colloidal particles (in COL) is responsible for the higher stability of foam prepared with the MPCM fraction. The smaller proteins (present in SUP) quickly adsorb at the air-water interface, ensuring a small bubble size, and subsequently, they form a stiff viscoelastic film to stabilize the bubbles against coalescence. The colloidal-sized particles (in COL) block the lamellae and Plateau borders, slowing down the drainage rate, and providing additional stability to the foam. This mechanism is illustrated in Fig. 9. A similar mechanism was also shown for casein micelle dispersions, studied at 4 and 20 °C. The casein micelles at 4 °C formed a substantially weaker interfacial layer than at 20 °C, but the foam stabilised with casein micelles at 4 °C was about 7 times more stable with a foam half-life time of >24 h than the same micelles studied at 20 °C. This work showed that the casein micelles formed larger particles at a colder temperature, leading to thicker and more stable thin films, and thus giving the earlier mentioned particle-based stabilisation of the foam (Chen et al., 2017).

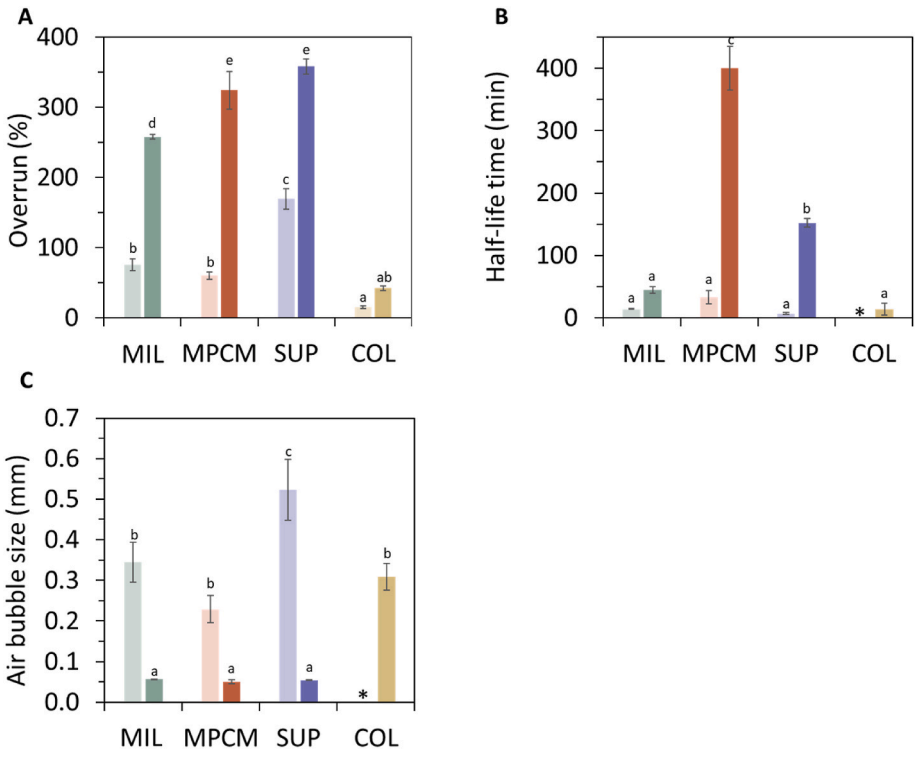

Fig. 8. The **A)** overrun, **B)** half-life time and **C)** air bubble size ($d_{3,2}$) of MIL (mildly purified mung bean protein mixture), MPCM (mung bean protein colloids mixture), SUP (supernatant) and COL (pellets) stabilised foam. Foams were prepared at protein concentration of 0.1 wt% (light colour bars) and 1 wt% (dark colour bars). The average and standard deviations were obtained from at least 3 replicates. * 0.1 wt% COL foams were not created for half-life time and air bubble size analysis.

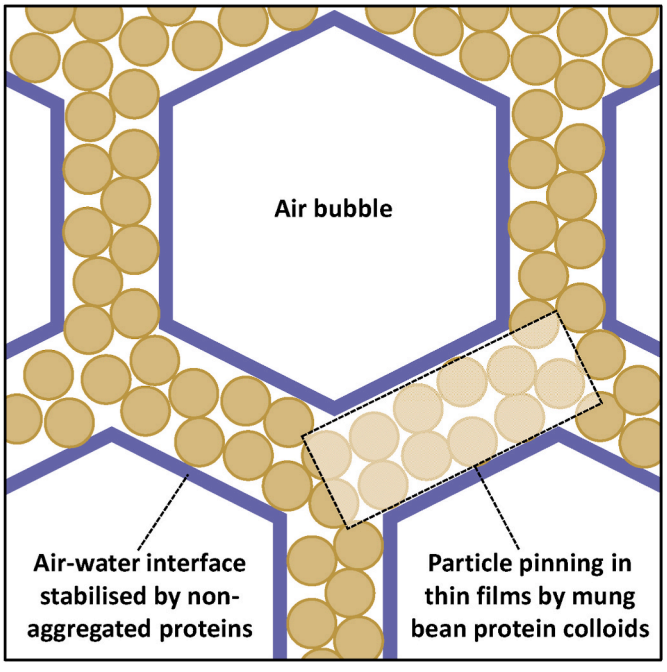

Fig. 9. Simplified schematic overview of MPCM (mung bean protein colloids mixtures) stabilised foam.

4. Conclusions

The interfacial behaviour of mung bean protein colloids mixtures (MPCM) and their fractions were studied to reveal the mechanism behind the MPCM's excellent foaming properties. The SUP fraction seems to dominate interfacial behaviour of MPCM, since they both were found to form similarly stiff layers at the air-water interface. The colloid (COL) fraction presented a distinctly more stretchable and weaker interface compared to the supernatant (SUP) fraction. This could be attributed to its relatively larger particle size, which resulted in slow interface adsorption, most likely by small amounts of non-aggregated proteins still present in the sample. AFM images could not confirm the presence of significant amounts of COL particles at the interface.

In foam tests, MPCM showed both high foam capacity (app. 325%) and foam stability (app. 400 min). The small and non-aggregated proteins in the MPCM appear to be responsible for the formation of stiff air-water interfaces, leading to the rapid formation of small air bubbles, thus giving high foam capacity. The colloids in the MPCM showed slow adsorption and poor air bubble formation, but possessed the ability to block the thin films between air bubbles and Plateau borders, and may even have caused pinning of the thin films. This decreased the drainage rate and led to high foam stability for the MPCM sample. The colloids and non-aggregated protein fraction hence co-operate in the formation of highly stable MPCM foam. Heat-induced aggregates can enhance the foaming stability of mung bean proteins as for other previously reported plant-based proteins and dairy proteins, and also lead to a foam with high capacity and stability. Hence, MPCM can be considered a promising and novel foaming agent and hydrocolloid for plant-based food products, for example, protein-fortified beverages.

CRediT authorship contribution statement

Qiuhuizi Yang: Writing – review & editing, Writing – original draft, Visualization, Investigation, Formal analysis, Data curation. **Jack Yang:** Writing – review & editing, Visualization, Investigation, Formal analysis, Data curation, Conceptualization. **Babet Waterink:** Investigation, Formal analysis, Data curation. **Paul Venema:** Writing – review & editing, Supervision, Conceptualization. **Renko de Vries:** Writing –

review & editing, Supervision, Conceptualization. **Leonard M.C. Sagis:** Writing – review & editing, Supervision.

Declaration of competing interest

The authors have declared that no competing interest exist. This manuscript has not been published and is not under consideration for publication in any other journal. All authors approve this manuscript and its submission to Food Hydrocolloids.

Data availability

Data will be made available on request.

Acknowledgements

The authors appreciate the support from Helene C.M. Mocking-Bode for her contribution to the SEC results, which was conducted at the Wageningen University. Q. Yang acknowledges funding by the Chinese Scholarship Council (CSC). J. Yang acknowledges funding by TiFN, a public-private partnership on precompetitive research in food and nutrition. This research was per-formed with additional funding from the Netherlands Organisation for Scientific Research (NWO), and the Top Consortia for Knowledge and Innovation of the Dutch Ministry of Economic Affairs (TKI). NWO project number: ALWTF.2016.001.

References

Assatory, A., Vitelli, M., Rajabzadeh, A. R., & Legge, R. L. (2019). Dry fractionation methods for plant protein, starch and fiber enrichment: A review. *Trends in Food Science & Technology, 86*, 340–351. https://doi.org/10.1016/j.tifs.2019.02.006

Brishti, F. H., Zarei, M., Muhammad, S. K. S., & Saari, N. (2017). *Evaluation of the functional properties of mung bean.* pdf>.

Chen, M., Feijen, S., Sala, G., Meinders, M. B. J., van Valenberg, H. J. F., van Hooijdonk, A. C. M., & van der Linden, E. (2018). Foam stabilized by large casein micelle aggregates: The effect of aggregate number in foam lamella. *Food Hydrocolloids, 74*, 342–348. https://doi.org/10.1016/j.foodhyd.2017.08.026

Chen, M., Sala, G., Meinders, M. B. J., van Valenberg, H. J. F., van der Linden, E., & Sagis, L. M. C. (2017). Interfacial properties, thin film stability and foam stability of casein micelle dispersions. *Colloids and Surfaces B: Biointerfaces, 149*, 56–63. https://doi.org/10.1016/j.colsurfb.2016.10.010

Esmaeili, M., Rafe, A., Shahidi, S. A., & Ghorbani Hasan-Saraei, A. (2015). Functional properties of rice bran protein isolate at different pH levels. *Cereal Chemistry, 93*(1), 58–63. https://doi.org/10.1094/cchem-04-15-0078-r

Guo, F., Xiong, Y. L., Qin, F., Jian, H., Huang, X., & Chen, J. (2015). Surface properties of heat-induced soluble soy protein aggregates of different molecular masses. *Journal of Food Science, 80*(2), C279–C287. https://doi.org/10.1111/1750-3841.12761

Hou, D., Yousaf, L., Xue, Y., Hu, J., Wu, J., Hu, X., Feng, N., & Shen, Q. (2019). Mung bean (vigna radiata L.): Bioactive polyphenols, polysaccharides, peptides, and health benefits. *Nutrients, 11*(6). https://doi.org/10.3390/nu11061238

Inthavong, W., Chassenieux, C., & Nicolai, T. (2019). Viscosity of mixtures of protein aggregates with different sizes and morphologies [10.1039/C9SM00298G]. *Soft Matter, 15*(23), 4682–4688. https://doi.org/10.1039/C9SM00298G

Iriti, M., & Varoni, E. M. (2017). Pulses, healthy, and sustainable food sources for feeding the planet. *International Journal of Molecular Sciences, 18*(2). https://doi.org/10.3390/ijms18020255

Kornet, R., Yang, J., Venema, P., van der Linden, E., & Sagis, L. M. C. (2022). Optimizing pea protein fractionation to yield protein fractions with a high foaming and emulsifying capacity. *Food Hydrocolloids, 126*. https://doi.org/10.1016/j.foodhyd.2021.107456

Liu, F. F., Li, Y. Q., Wang, C. Y., Liang, Y., Zhao, X. Z., He, J. X., & Mo, H. Z. (2022). Physicochemical, functional and antioxidant properties of mung bean protein enzymatic hydrolysates. *Food Chemistry, 393*, Article 133397. https://doi.org/10.1016/j.foodchem.2022.133397

Ma, Z., Boye, J. I., Simpson, B. K., Prasher, S. O., Monpetit, D., & Malcolmson, L. (2011). Thermal processing effects on the functional properties and microstructure of lentil, chickpea, and pea flours. *Food Research International, 44*(8), 2534–2544. https://doi.org/10.1016/j.foodres.2010.12.017

Nicolai, T. (2016). Formation and functionality of self-assembled whey protein microgels. *Colloids and Surfaces B: Biointerfaces, 137*, 32–38. https://doi.org/10.1016/j.colsurfb.2015.05.055

Nicorescu, I., Loisel, C., Riaublanc, A., Vial, C., Djelveh, G., Cuvelier, G., & Legrand, J. (2009). Effect of dynamic heat treatment on the physical properties of whey protein foams. *Food Hydrocolloids, 23*(4), 1209–1219. https://doi.org/10.1016/j.foodhyd.2008.09.005

Nicorescu, I., Vial, C., Loisel, C., Riaublanc, A., Djelveh, G., Cuvelier, G., & Legrand, J. (2010). Influence of protein heat treatment on the continuous production of food foams. *Food Research International, 43*(6), 1585–1593. https://doi.org/10.1016/j.foodres.2010.03.015

Pelgrom, P. J. M., Boom, R. M., & Schutyser, M. A. I. (2015). Functional analysis of mildly refined fractions from yellow pea. *Food Hydrocolloids, 44*, 12–22. https://doi.org/10.1016/j.foodhyd.2014.09.001

Rühs, P. A., Affolter, C., Windhab, E. J., & Fischer, P. (2013). Shear and dilatational linear and nonlinear subphase controlled interfacial rheology of β-lactoglobulin fibrils and their derivatives. *Journal of Rheology, 57*(3), 1003–1022. https://doi.org/10.1122/1.4802051

Rullier, B., Axelos, M. A., Langevin, D., & Novales, B. (2009). Beta-lactoglobulin aggregates in foam films: Correlation between foam films and foaming properties. *Journal of Colloid and Interface Science, 336*(2), 750–755. https://doi.org/10.1016/j.jcis.2009.04.034

Rullier, B., Axelos, M. A., Langevin, D., & Novales, B. (2010). Beta-lactoglobulin aggregates in foam films: Effect of the concentration and size of the protein aggregates. *Journal of Colloid and Interface Science, 343*(1), 330–337. https://doi.org/10.1016/j.jcis.2009.11.015

Rullier, B., Novales, B., & Axelos, M. A. V. (2008). Effect of protein aggregates on foaming properties of β-lactoglobulin. *Colloids and Surfaces A: Physicochemical and Engineering Aspects, 330*(2–3), 96–102. https://doi.org/10.1016/j.colsurfa.2008.07.040

Sagis, L. M. C., Liu, B., Li, Y., Essers, J., Yang, J., Moghimikheirabadi, A., Hinderink, E., Berton-Carabin, C., & Schroen, K. (2019). Dynamic heterogeneity in complex interfaces of soft interface-dominated materials. *Scientific Reports, 9*(1), 2938. https://doi.org/10.1038/s41598-019-39761-7

Sağlam, D., Venema, P., de Vries, R., & van der Linden, E. (2013). The influence of pH and ionic strength on the swelling of dense protein particles [10.1039/C3SM50170A]. *Soft Matter, 9*(18), 4598–4606. https://doi.org/10.1039/C3SM50170A

Sah, B. K., & Kundu, S. (2017). Modification of hysteresis behaviors of protein monolayer and the corresponding structures with the variation of protein surface charges. *Colloids and Surfaces B: Biointerfaces, 159*, 696–704. https://doi.org/10.1016/j.colsurfb.2017.08.032

Saint-Jalmes, A., Peugeot, M. L., Ferraz, H., & Langevin, D. (2005). Differences between protein and surfactant foams: Microscopic properties, stability and coarsening. *Colloids and Surfaces A: Physicochemical and Engineering Aspects, 263*(1–3), 219–225. https://doi.org/10.1016/j.colsurfa.2005.02.002

Sandoval-Castilla, O., Lobato-Calleros, C., Aguirre-Mandujano, E., & Vernon-Carter, E. J. (2004). Microstructure and texture of yogurt as influenced by fat replacers. *International Dairy Journal, 14*(2), 151–159. https://doi.org/10.1016/S0958-6946(03)00166-3

Schmitt, C., Bovay, C., Rouvet, M., Shojaei-Rami, S., & Kolodziejczyk, E. (2007). Whey protein soluble aggregates from heating with NaCl: Physicochemical, interfacial, and foaming properties. *Langmuir, 23*(8), 4155–4166. https://doi.org/10.1021/la0632575

Shen, L., & Tang, C.-H. (2012). Microfluidization as a potential technique to modify surface properties of soy protein isolate. *Food Research International, 48*(1), 108–118. https://doi.org/10.1016/j.foodres.2012.03.006

Shewan, H. M., & Stokes, J. R. (2013). Review of techniques to manufacture micro-hydrogel particles for the food industry and their applications. *Journal of Food Engineering, 119*(4), 781–792. https://doi.org/10.1016/j.jfoodeng.2013.06.046

Wang, Z., Li, Y., Jiang, L., Qi, B., & Zhou, L. (2014). Relationship between secondary structure and surface hydrophobicity of soybean protein isolate subjected to heat treatment. *Journal of Chemistry, 2014*, 1–10. https://doi.org/10.1155/2014/475389

Wang, Y., Zhao, J., Zhang, S., Zhao, X., Liu, Y., Jiang, J., & Xiong, Y. L. (2022). Structural and rheological properties of mung bean protein emulsion as a liquid egg substitute: The effect of pH shifting and calcium. *Food Hydrocolloids, 126*. https://doi.org/10.1016/j.foodhyd.2022.107485

Xia, W., Botma, T. E., Sagis, L. M. C., & Yang, J. (2022). Selective proteolysis of β-conglycinin as a tool to increase air-water interface and foam stabilising properties of soy proteins. *Food Hydrocolloids, 130*. https://doi.org/10.1016/j.foodhyd.2022.107726

Yang, J., Berton-Carabin, C. C., Nikiforidis, C. V., van der Linden, E., & Sagis, L. M. C. (2022). Competition of rapeseed proteins and oleosomes for the air-water interface and its effect on the foaming properties of protein-oleosome mixtures. *Food Hydrocolloids, 122*, Article 107078. https://doi.org/10.1016/j.foodhyd.2021.107078

Yang, Q., Eikelboom, E., van der Linden, E., de Vries, R., & Venema, P. (2022). A mild hybrid liquid separation to obtain functional mungbean protein. *Lwt, 154*. https://doi.org/10.1016/j.lwt.2021.112784

Yang, J., Faber, I., Berton-Carabin, C. C., Nikiforidis, C. V., van der Linden, E., & Sagis, L. M. C. (2021). Foams and air-water interfaces stabilised by mildly purified rapeseed proteins after defatting. *Food Hydrocolloids, 112*. https://doi.org/10.1016/j.foodhyd.2020.106270

Yang, J., Kornet, R., Diedericks, C. F., Yang, Q., Berton-Carabin, C. C., Nikiforidis, C. V., Venema, P., van der Linden, E., & Sagis, L. M. C. (2022). Rethinking plant protein extraction: Albumin—from side stream to an excellent foaming ingredient. *Food Structure, 31*. https://doi.org/10.1016/j.foostr.2022.100254

Yang, J., Lamochi Roozalipour, S. P., Berton-Carabin, C. C., Nikiforidis, C. V., van der Linden, E., & Sagis, L. M. C. (2021). Air-water interfacial and foaming properties of whey protein - sinapic acid mixtures. *Food Hydrocolloids, 112*. https://doi.org/10.1016/j.foodhyd.2020.106467

Yang, J., Mocking-Bode, H. C. M., van den Hoek, I. A. F., Theunissen, M., Voudouris, P., Meinders, M. B. J., & Sagis, L. M. C. (2022). The impact of heating and freeze or spray drying on the interface and foam stabilising properties of pea protein extracts:

Explained by aggregation and protein composition. *Food Hydrocolloids, 133*. https://doi.org/10.1016/j.foodhyd.2022.107913

Yang, J., Thielen, I., Berton-Carabin, C. C., van der Linden, E., & Sagis, L. M. C. (2020). Nonlinear interfacial rheology and atomic force microscopy of air-water interfaces stabilized by whey protein beads and their constituents. *Food Hydrocolloids, 101*. https://doi.org/10.1016/j.foodhyd.2019.105466

Yang, Q., Venema, P., van der Linden, E., & de Vries, R. (2023). Soluble protein particles produced directly from mung bean flour by simple coacervation. *Food Hydrocolloids*. , Article 108541. https://doi.org/10.1016/j.foodhyd.2023.108541

Yang, J., Yang, Q., Waterink, B., Venema, P., de Vries, R., & Sagis, L. M. C. (2023). Physical, interfacial and foaming properties of different mung bean protein fractions. *Food Hydrocolloids, 143*. https://doi.org/10.1016/j.foodhyd.2023.108885